Estimating population size by spatially explicit capture–recapture

Murray G. Efford and Rachel M. Fewster

M. G. Efford (murray.efford@gmail.com), 60 Helensburgh Road, Dunedin 9010, New Zealand. – R. M. Fewster, Dept of Statistics, Univ. of Auckland, Private Bag 92019, Auckland, New Zealand.

The number of animals in a population is conventionally estimated by capture–recapture without modelling the spatial relationships between animals and detectors. Problems arise with non-spatial estimators when individuals differ in their exposure to traps or the target population is poorly defined. Spatially explicit capture–recapture (SECR) methods devised recently to estimate population density largely avoid these problems. Some applications require estimates of population size rather than density, and population size in a defined area may be obtained as a derived parameter from SECR models. While this use of SECR has potential benefits over conventional capture–recapture, including reduced bias, it is unfamiliar to field biologists and no study has examined the precision and robustness of the estimates. We used simulation to compare the performance of SECR and conventional estimators of population size with respect to bias and confidence interval coverage for several spatial scenarios. Three possible estimators for the sampling variance of realised population size all performed well. The precision of SECR estimates was nearly the same as that of the null-model conventional population estimator. SECR estimates of population size were nearly unbiased (relative bias 0–10%) in all scenarios, including surveys in randomly generated patchy landscapes. Confidence interval coverage was near the nominal level. We used SECR to estimate the population of a species of skink *Oligosoma infrapunctatum* from pitfall trapping. The estimated number in the area bounded by the outermost traps differed little between a homogeneous density model and models with a quadratic trend in density or a habitat effect on density, despite evidence that the latter models fitted better. Extrapolation of trend models to a larger plot may be misleading. To avoid extrapolation, a large region of interest should be sampled throughout, either with one continuous trapping grid or with clusters of traps dispersed widely according to a probability-based and spatially representative sampling design.

The size of many animal populations must be assessed indirectly because their secretive habits render a direct count impossible. Capture–recapture is the primary indirect method and has a central place in the ecological toolkit. Repeated samples are drawn from the population of interest; animals are marked so that individuals may be distinguished and returned to mix with the population. Data for each captured individual may be summarized as a 'capture history', a record of capture and non-capture in successive samples. Statistical modelling of capture histories leads to an estimate of the unsampled fraction of the population and hence the total number. New technology that exploits natural marks, such as microsatellite DNA or individual pelage patterns captured on automatic cameras, has removed the need for physical capture in many situations, so capture–recapture methods are now applied to a greater range of species than ever before.

Statistical methodologies for estimating population size from the capture histories of trapped animals were detailed by Otis et al. (1978) and implemented in the software CAPTURE. Methods in widespread use have since changed only incrementally. Specific advances have been the flexible modelling of individual-level covariates of detection probability (Huggins 1989), model selection and model averaging using AIC (Burnham and Anderson 2002), finite and continuous mixtures to allow for unmodelled individual heterogeneity (Pledger 2000, Dorazio and Royle 2003), and general use of the software MARK as a framework for modelling with covariates and constraints (White and Burnham 1999, White 2005).

The last few years have seen progress on the related problem of estimating population density (Efford 2004, Borchers and Efford 2008, Royle and Young 2008), defining a set of methods known as spatially explicit capture–recapture (SECR). Density estimation was previously an add-on to capture–recapture: given an estimate of population size (N) and the 'effective trapping area' A, an estimate of density is $\hat{D} = \hat{N}/A$. However, there is neither adequate theory to define A independently of this equation nor a reliable estimator. SECR provides a unified theory in which population density D is integral to the fitted model. The essential features of SECR are a model for the spatial distribution of home-range centres and a model of distance-dependent detection. The model for home-range centres is a spatial point process that is 'latent' in the data: we can determine properties such as its density by fitting a

model, without observing individual home-range centres. Decline in detection probability with the distance between a detector and a home range centre can likewise be inferred from the clumping of locations at which each individual is observed. This requires that some individuals are detected at multiple locations. Models may be fitted by simulation and inverse prediction (Efford 2004), likelihood maximization (Borchers and Efford 2008) or Markov chain Monte Carlo (MCMC) methods (Royle and Young 2008, Gardner et al. 2009).

Population density is a useful parameter for many ecological purposes. However, population size, the absolute number of distinct individuals, is often needed in particular applications such as the management of harvested or declining populations. This has been the domain of conventional non-spatial capture–recapture methods (Chao and Huggins 2005a, b). However, N, defined as the number of individuals in a geographic region, is also available from spatially explicit models. To estimate N we first fit a SECR model and then infer the number of individuals from the model. There are potential advantages in such a spatial approach at three levels. Firstly, SECR automatically allows for heterogeneity among individuals in their exposure to detectors, which removes a key source of bias in non-spatial estimators. Secondly, the estimate of N relates to a specified geographical region rather than a notional 'effective trapping area' with no geographical boundary. Thirdly, SECR accommodates designs in which sampling is not continuous across space (i.e. contains 'holes').

While the possibility of using SECR in this way appears in the methodological literature along with commentary on the advantages of SECR models (Borchers and Efford 2008, Gardner et al. 2009), there has been little uptake by biologists. The force of the argument in the preceding paragraph remains unclear because no comparison has been published of the performance of spatial and non-spatial estimators of N and the robustness of spatial estimators has not been established. Fitting a more complex model would seem to risk loss of precision. Further, the default estimates of sampling error from some software for SECR (Efford et al. 2004, Efford 2012) should not be compared directly to errors from common non-spatial methods (Otis et al. 1978) as the former include spatial process variance.

In this note we set out the necessary theory for estimating population size in an arbitrary region from SECR models, and compare estimates under the spatial and non-spatial approaches using an example dataset and simulations. Which approach is more appropriate may be expected to depend on the spatial extent of sampling and the extent of the habitat occupied by the target population. We therefore assessed the accuracy of spatial and non-spatial estimates of population size for datasets simulated under four scenarios differing in the spatial extent of sampling relative to a single continuous patch of occupied habitat. Real landscapes are often irregular mosaics, part unsuitable and part potentially occupied by the target species. If the part that is potentially occupied cannot be predicted from covariates then existing Poisson-based SECR models are not strictly appropriate. Patchiness of this sort may be common, and it is desirable that estimators of population size are robust when, for example, a spatially homogeneous model is fitted

to a distribution that, unknown to the researcher, is spatially heterogeneous. We tested the robustness of population estimators in this case using randomly generated habitat maps.

The ability to estimate N from an SECR model can lead to major improvements and efficiencies in study design. This is foreshadowed in one of the simulated scenarios, and outlined in the Discussion.

Non-spatial and spatial concepts of population size

The state variable in a conventional non-spatial capture–recapture model is an integer number of individuals comprising the population of interest. Sampling must be arranged so that all individuals in the population have non-zero probability of capture. In many studies the logic is reversed: a sampling design (e.g. a trapping grid) is established, and the population of interest is defined as those individuals with a non-zero probability of capture (see examples in Otis et al. 1978). This has been a persistent weakness of non-spatial methods applied to spatial capture–recapture data from unbounded populations, as the target population implicitly varies with the conditions of observation. Specifically, home-range size and trapping efficiency and duration together determine the number of marginal animals that meet an implied threshold of minimum capture probability, and are therefore part of the target population (Efford et al. 2004).

The state variable in spatially explicit capture–recapture is a spatial point process. Each point represents an individual home-range centre. For computational convenience a Poisson process is often assumed; the intensity of the process may vary over space, in which case it is described as 'inhomogeneous'. The fitted density model may be visualized as a surface of varying height, for which we use the notation $D(\mathbf{x}; \phi)$ where $\mathbf{x}$ is a point in two dimensions (a vector of x–y coordinates) and ϕ is a vector of parameters. In almost all applications to date the fitted surface has been flat, so ϕ corresponds to a single parameter, the population density. Estimating the height of the surface does not, in principle, require knowledge of its extent, although for estimation it is convenient to consider a delimited and finite 'region of integration' (Borchers and Efford 2008). We use the symbol S for this region. The term 'state space' was used by Royle and Young (2008) for an equivalent region in the context of simulation-based estimation. Animals with home-range centres outside S, if they exist, have negligible chance of getting caught and may be ignored in computations. The region need not be contiguous and may exclude areas of non-habitat near the detectors that are known a priori to contain no home-range centres of the species. The analyst is free to specify S; estimates will be biased if S is so small that some caught animals have home-range centres outside S.

In this paper we consider the population of individuals with home-range centres in a defined geographic region B. This is most easily calculated when B and S coincide, but B may be any region to which the model $D(\mathbf{x}; \phi)$ applies, by assumption or design. The conditions under which the model provides valid inference for B is a question to which we return briefly in the Discussion. More mathematical notation and details of estimation follow in Methods.

Expected and realised population size

Non-spatial closed population estimation has long contained two parallel views or models of population size, as described eloquently by Sandland and Cormack (1984). These may be characterized (equivalently) as Poisson vs multinomial or unconditional vs conditional or random-N vs fixed-N or expected-N vs realised-N (Sandland and Cormack 1984, Johnson et al. 2010). The distinction rests on whether the state model includes process variation in N or treats N as fixed. Most ecologists have embraced the 'fixed-N' view represented by Otis et al. (1978) and many subsequent authors, but development has continued of Cormack's Poisson log-linear models that incorporate random variation in N (Rivest and Baillargeon 2007). The main practical difference is that conditioning on N excludes process uncertainty from the sampling variance. The same possibilities exist for computing the sampling variance of population size estimated from spatial models, and it is important when comparing the precision of spatial and non-spatial estimators that the sampling errors are compatible in this sense. In the treatment below we use the 'expected-N' (μ) vs 'realised-N' terminology of Johnson et al. (2010); where N is used without qualification it refers to realised N. Alternative expressions for sampling error are given for when spatial process variance is included (expected N) or excluded (realised N). The latter allows comparison with the estimators of Otis et al. (1978) and is appropriate when inference is limited to the realised population in a particular region.

Methods

SECR models were fitted by maximizing the full likelihood (see Appendix 1 for comments on Bayesian methods). The SECR observation model describes the probability of detection at each detector as a function of distance, with parameter vector θ (for a half-normal function, θ comprises the intercept g_0 and scale σ). The concatenation of ϕ and θ is the vector β comprising all parameters of the model, some or all of which may be estimated on a transformed (link) scale. Maximization of the likelihood yields estimates of the β parameters and their asymptotic variance-covariance matrix $\mathbf{V}$ (Borchers and Efford 2008, Efford et al. 2009a). We use the notation $p.(\mathbf{x}; \theta)$ for the probability that an animal is caught at least once; for a given set of detectors, $p.(\mathbf{x}; \theta)$ depends on the home-range location $\mathbf{x}$, the detection parameters, and the duration of sampling (for the specific form of this function see e.g. Efford et al. 2009a).

Expected number in an arbitrary region

Suppose we want to estimate the number of range centres N within a geographical boundary that defines an arbitrary region B. If density is described by an inhomogeneous Poisson model $D(\mathbf{x}; \phi)$ then N has a Poisson distribution. If D is also constant over space (i.e. the density surface is flat) and the region has area A_B then estimates of the expected number μ and its sampling variance are multiples of the corresponding density estimates: $\bar{\mu} = A_B \widehat{D}$ and

$\widehat{\mathrm{var}}[\bar{\mu}] = A_B^2 \widehat{\mathrm{var}}(\widehat{D})$. More generally, the expected number is given by the volume under the density surface:

$$E[N] = \mu = \int_B D(\mathbf{x}; \phi) \, \mathbf{dx} \tag{1}$$

estimated by substituting an estimate of ϕ. Two-dimensional integration may be performed numerically by summing over discrete pixels chosen to be small enough that discretisation has negligible effect on the estimates. The sampling variance of $\hat{\mu}$ is estimated numerically from $\widehat{\mathbf{V}}$ as

$$\widehat{\mathrm{var}}[\bar{\mu}] = \widehat{\mathbf{G}}^{\mathrm{T}} \widehat{\mathbf{V}} \widehat{\mathbf{G}} \tag{2}$$

where the vector $\widehat{\mathbf{G}}$ is the gradient of $\bar{\mu}$ with respect to β, evaluated numerically at the maximum likelihood estimates of β. Modelling temporal variation in D (e.g. as trend across sessions; Efford et al. 2009a) is directly equivalent to modelling temporal variation in μ, assuming no temporal change in spatial distribution across the region.

Realised number in an arbitrary region

If region B contains the range centres of all n individuals observed, which is implied if S is contained within B, then an estimate of the realised N is given by the sum of animals actually observed and those predicted to be present under the model, but not observed:

$$\widehat{N} = n + \int_B D(\mathbf{x}; \widehat{\phi})[1 - p.(\mathbf{x}; \widehat{\theta})] \, \mathbf{dx} \tag{3}$$

Estimates of the realised and expected number are approximately the same ($\widehat{N} = \bar{\mu}$) when D is constant (using $E[n] = \int_S D(\mathbf{x}; \phi)p.(\mathbf{x}; \theta)\mathbf{dx}$, and taking D outside the integrals). However, $\widehat{N}$ has smaller sampling variance than $\bar{\mu}$ because uncertainty is confined to the unobserved fraction represented by the integral in Eq. 3 (Johnson et al. (2010) noted the analogy to adjusting for a finite population in conventional sampling). We considered three ways to estimate the sampling variance of realised N, i.e. $\widehat{\mathrm{var}}(\widehat{N}|N)$ (Appendix 2). In the first, n is treated as a binomial variable of size N, rather than a Poisson variable as in the main model; maximization of the likelihood (Borchers and Efford 2008, p. 379) leads to asymptotic variance estimates for the realised (fixed) N. This is the most direct method, but it requires that B = S (the region of interest coincides with the region of integration). Two further methods allow B ≥ S. One uses an approximation to the mean squared prediction error from Johnson et al. (2010). The other method is derived from the law of total variance and the assumption that N is Poisson-distributed:

$$\widehat{\mathrm{var}}(\widehat{N}|N) = \widehat{\mathrm{var}}(\bar{\mu}) - \bar{\mu}. \tag{4}$$

All three variance estimators performed adequately with simulated data (Appendix 2). We used Eq. 4 in later analyses as it is simple and fast to apply given an estimate of $\widehat{\mathrm{var}}(\bar{\mu})$ from Eq. 2.

Confidence intervals

A symmetrical interval for $\widehat{N}$ based on variance estimates from the previous section may have lower bound less than n. In practice it is useful to define an asymmetrical lognormal

interval for $\widehat{N}$ with n as a lower bound, following the procedure commonly used in non-spatial analyses (Rexstad and Burnham 1991). Such an interval is $[n + (\widehat{N} - n)/C,$

$n + (\widehat{N} - n) \times C]$, where $C = \exp\left(1.96\sqrt{\log\left[1 + \dfrac{\widehat{\text{var}}\,(\widehat{N})}{(\widehat{N} - n)^2}\right]}\right)$,

and 1.96 is the standard normal deviate corresponding to a 95% interval. An asymmetrical lognormal interval is also appropriate for $\hat{\mu}$, although in that case the lower bound is zero and the interval is $[\hat{\mu}/C', \hat{\mu} \times C']$, where $C' = \exp\left(1.96\sqrt{\log\left[1 + \widehat{\text{var}}\,(\hat{\mu})/\hat{\mu}^2\right]}\right)$, which is equivalent to back-transforming symmetrical limits from the log scale. We later provide evidence from simulations that such intervals have coverage acceptably close to the nominal 95% level.

Scenarios for simulated spatial sampling

We considered four scenarios for the spatial extent of sampling in relation to an elliptical area of habitat occupied by the target population. The first (scenario A) represents an isolated island of habitat sampled throughout with detectors spaced so there are no 'holes' between detectors large enough to contain a home range (Fig. 1a). In this scenario all animals were exposed to risk of capture. In a second scenario (B), the detector array sampled only part of a more extensive biological population, whose members therefore differed greatly in exposure to detectors (Fig. 1b). The boundary in Fig. 1b represented either the known extent of the occupied habitat or the extent of a region of interest such as a management unit. In a third scenario (C), the population occupied an unknown part of a larger region, and detectors were distributed without 'holes' across the entire region (Fig. 1c). In design (D) detectors were distributed across the area of

the larger population in clusters placed systematically, with a random origin, to obtain a spatially representative sample; clusters lying partly outside the region were omitted (Fig. 1d). The pattern of recaptures within a cluster provides information on the scale of detection. The number of detectors differed between scenarios (69, 64, 255, 72). Scenarios A and C satisfied the design requirement for non-spatial estimation that all individuals were at risk of capture, whereas with the chosen detection parameters (below) some animals in scenarios B and D had near-zero detection probability.

Detectors were spaced 100 m apart. The simulated population density was uniform (1 ha^{-1}) throughout the shaded elliptical areas in Fig. 1, and the realised population size followed a Poisson distribution over replicates. Sampling was simulated over 5 occasions with a half-normal detection function ($g_0 = 0.2$, $\sigma = 50$ m) using a competing risks model for multi-catch traps (Borchers and Efford 2008). The expected distribution of individual detection probabilities (p_i) was approximated by computing $p(\mathbf{x})$ (for a single occasion) and $p.(\mathbf{x})$ (for the entire experiment) at points on a 5×5 m grid across each habitat ellipse (Table 1). Heterogeneity was summarized as the coefficient of variation of $p(\mathbf{x})$ and $p.(\mathbf{x})$. Three closed-population estimators from Otis et al. (1978) were computed for each dataset (the null estimator for model M_0, the Zippin estimator for model M_b, and the Burnham and Overton (1978) jackknife estimator for model M_h). Likelihood-based estimators for model M_h, specifically the two-class finite mixture estimator (Pledger 2000) and the beta-binomial estimator (Dorazio and Royle 2003), were not used as some simulations produced unrealistic estimates or the variance computation failed, making it difficult to report the simulation results consistently (see also discussion in Pledger 2005).

SECR models were fitted using as region of integration either the 'known' extent of the habitat ellipse (scenarios A,
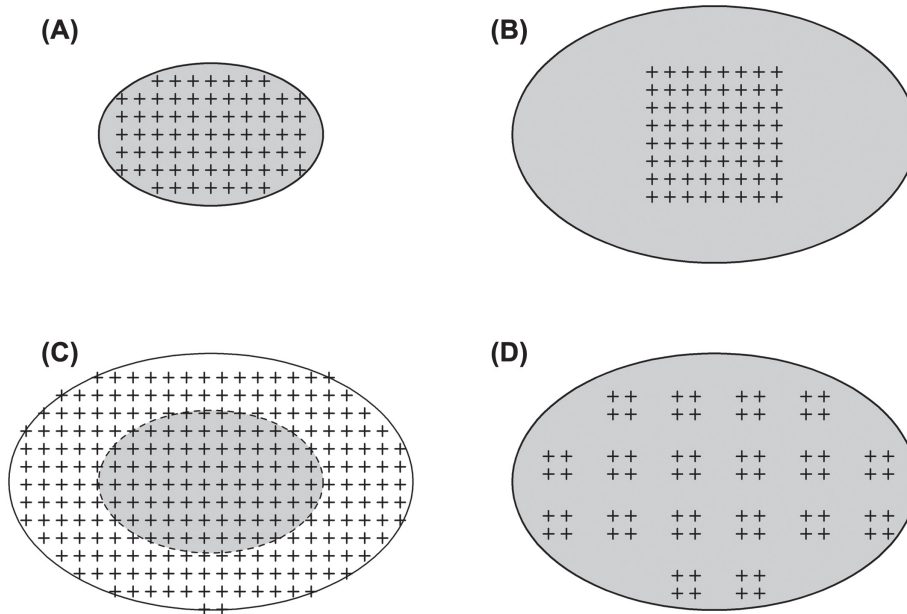

Figure 1. Scenarios for simulations of spatial sampling. Shading indicates extent of occupied habitat. '+' trap sites. (A) Detectors throughout a habitat island. (B) Spatially unrepresentative, local sample of an extensive population. (C) Detectors placed evenly across a wide region, only some of which is occupied. (D) Spatially representative sample of an extensive population using a systematic array of detector clusters with random origin.

Table 1. Characteristics of simulated populations (see text for scenarios). μ is the expected number of individuals. E(n) and E(r) refer to the expected numbers of first captures and recaptures; $E(p_i)$ is the mean detection probability; $CV(p_i)$ measures heterogeneity in detection probability across individuals caused by differing exposure to traps. All E(n) and E(r), and all statistics for the Patchy scenario were from Monte Carlo simulations (10 000 replicates).

Scenario	μ	E(n)	E(r)	Single occasion		Overall	
				$E(p_i)$	$CV(p_i)$	$E(p_i)$	$CV(p_i)$
A	79.1	57.3	28.0	0.240	0.285	0.723	0.222
B	256.3	56.3	26.3	0.072	1.586	0.220	1.522
C	79.1	64.0	34.4	0.267	0.149	0.809	0.009
D	256.3	75.8	24.4	0.083	1.056	0.298	0.923
Patchy	175.3	136.0	70.4	0.266	0.146	0.779	0.105

B, D) or the ellipse that contained all detector locations in scenario C. Pixel width was 25 m. The fitted detection model was half-normal, as in the generating model. A homogeneous Poisson process was fitted by maximizing the full likelihood, with density on the log scale. Numerical estimates of the expected and realised population sizes and 95% lognormal confidence (prediction) intervals followed Eq. 1–4. Calculations used ver. 2.2.0 of the R package 'secr' (Efford 2012), specifically functions 'sim.capthist', 'secr.fit' and 'region.N'.

Performance of estimators was summarized as the average across replicates of relative bias ($RB_j = (\widehat{N}_j - N_j)/N_j$ where N_j was the true number in realisation j), and relative standard error ($RSE_j = \widehat{SE}(\widehat{N}_j)/\widehat{N}_j$), and as the coverage of N_j by the computed 95% intervals. An exception was made for the SECR estimate of expected population size μ: the bias and coverage of these estimates was expressed relative to the expected value of the known distribution (Table 1).

Simulations of patchy habitat

We tested the robustness of population estimates from a homogeneous SECR model when the population was

constrained to lie within random habitat patches comprising on average 25% of the landscape. Patches were generated by the modified random cluster algorithm of Saura and Martínez-Millán (2000) on a 64×64 grid and clipped to an elliptical boundary. The patch-fragmentation parameter ('initial probability') was set to 0.5, resulting in realisations such as those in Fig. 2. Home-range centres were distributed randomly at a density of 4 ha^{-1} within the simulated habitat (overall density 1 ha^{-1}). Spatial sampling and estimation were simulated using a grid of traps throughout the bounding ellipse, and estimation was carried out as before. True expected population size was obtained by averaging 10 000 simulations (mean 175.29, SE 0.74, CV 0.41). This value differed slightly from one computed directly from the ellipse area (178.01) owing to edge effects in the discrete-space habitat representation; the simulated mean was used for calculating bias in estimators.

Skink field study

Three diurnal lizard species were studied over several years on a steep bracken-covered hillside in the Upper Buller Valley, South Island, New Zealand. Pitfall traps (sunken cans baited with a morsel of fruit in sugar syrup) were set in two large grids, each with 231 traps about 5 m apart and operated intermittently through 1995–1996. Traps were checked daily and individuals were marked uniquely by toe clipping. We selected data on one species (*Oligosoma infrapunctatum*) from one grid run for 3 days in October 1995 (Fig. 3). Ground cover and vegetation were recorded for a 1-m radius plot at each trap site. Each site was assigned to one of two classes: 'low cover' (open with bare ground or low-canopy vegetation and grasses; 61.9% of sites) and 'high cover' (more-closed vegetation with a higher canopy; 38.1% of sites). The dataset is described further by Efford (2012).

We fitted competing-risk SECR models with a half-normal detection function by numerically maximizing the
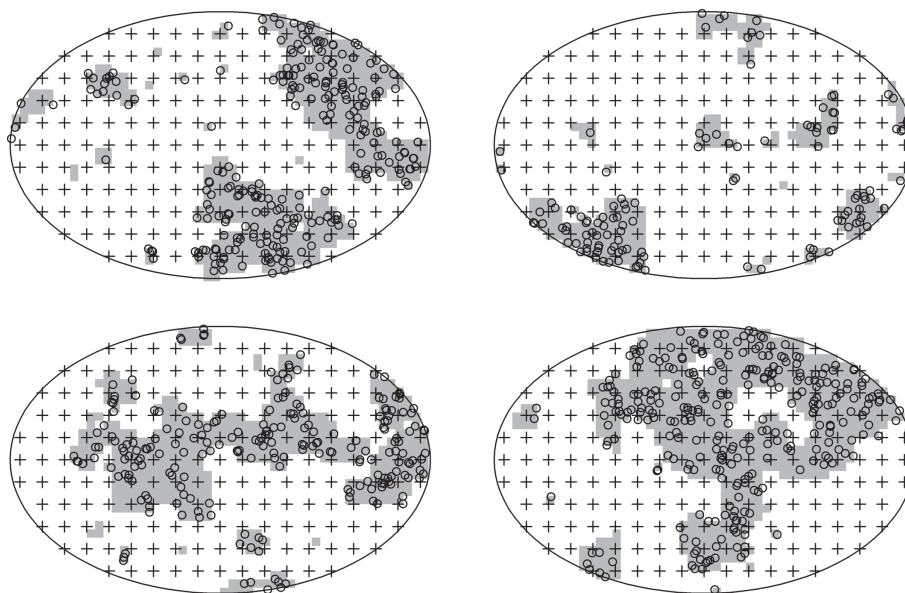

Figure 2. Random habitat maps (shaded) simulated by the algorithm of Saura and Martínez-Millán (2000) with expected coverage 25% and initial probability 0.5. Circles indicate simulated home-range centres (Poisson-distributed within habitat). '+' trap sites.
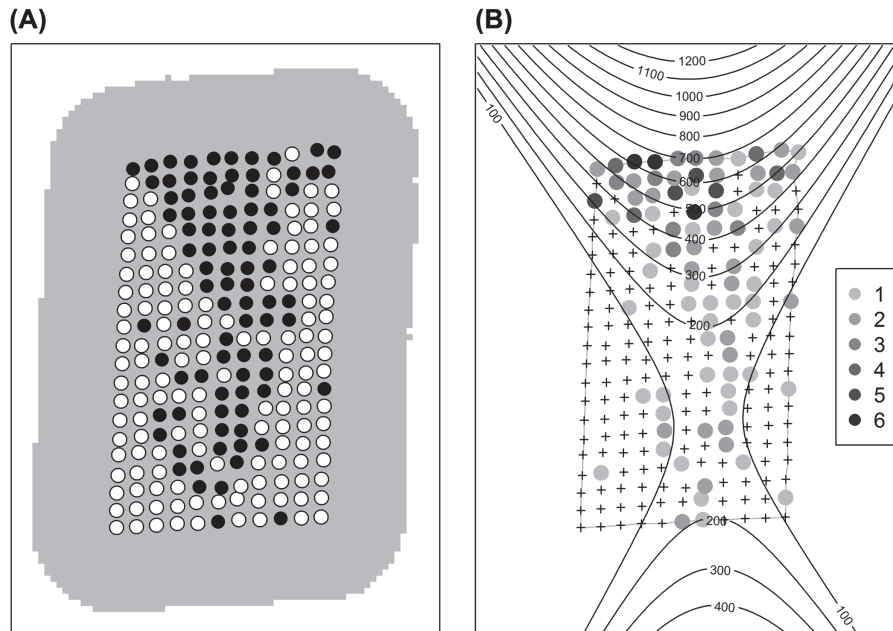
Figure 3. Skinks *Oligosoma infrapunctatum* sampled by pitfall trapping in the Buller Valley, South Island, New Zealand, in October 1995. (A) Trap sites (circles) and region of integration used to fit SECR models (shaded; area 1.08 ha). Two habitat types are distinguished: filled (black) trap sites were in areas of greater cover. (B) Number of skinks trapped at each site (shaded dots) and contours of population density predicted by a quadratic trend model (skinks ha^{-1}). Traps were about 5 m apart.

likelihood (Borchers and Efford 2008). The fitted density model was either flat ('Null'), allowed a distinct expected density for each habitat class ('Habitat'), or included a quadratic spatial trend ('Qtrend'). Trend in density was modelled on the natural scale, rather than log-transformed. This reduced the risk from extrapolation, but parameter values had to be scaled for numerical maximization. The region of integration comprised 5750 pixels, each 1.43 m², and extended 20 m beyond the traps (Fig. 3A); results were not affected by reduced pixel size or increased buffer width in post-hoc tests. The habitat class of each pixel in the region of integration was inferred from the nearest trap site if that was within 5 m. The habitat class of peripheral pixels (those further than 5 m from any trap) was assigned at random in proportion to the frequencies at trap sites.

Estimates of population size were obtained for two regions: the region of integration (shaded area in Fig. 3A) and the area enclosed by the perimeter traps (Fig. 3B). Expected and realised population sizes were estimated using Eq. 1–4. Bias and confidence interval coverage for the null-model estimates of realised number were checked with data simulated under the inhomogeneous models (1000 replicates).

Results

Simulations of spatial scenarios

The null and Zippin closed population estimators performed moderately well (low bias and near-nominal coverage) in scenarios A and C where almost all individuals had high probability of detection, although both estimators were negatively biased in scenario A, and the Zippin estimator

showed poor precision (Table 2). The jackknife estimator performed relatively poorly in all scenarios. As expected, conventional closed population estimators were very biased when some members of the target population were distant from detectors (scenarios B and D).

SECR estimates of population size were nearly unbiased (estimated relative bias less than 3%) and the coverage of intervals was near perfect for scenarios A and B (Table 2). The constant-density SECR estimator might have been expected to perform poorly when the region of integration included considerable unoccupied habitat (scenario C). Estimated bias in this instance was on the order of +5% and interval coverage of realised population size (88%) was below the nominal level. There were indications of slight positive bias in the SECR estimates for scenario D, but interval coverage (93–94%) remained near the nominal level. In scenarios where both null and SECR estimators provided nearly unbiased estimates, the estimated precision of realised population size from the null model was slightly better than that from SECR (RSE 0.090 vs 0.098 in scenario A, 0.075 vs 0.082 in scenario C).

We also calculated SECR estimates with spatial scale σ fixed to an arbitrary large value (10 000 m). This turns the spatial model into a non-spatial model. The results are not tabulated as both the estimates of N and their confidence limits were nearly indistinguishable from the equivalent null-model closed population estimates.

Simulations of patchy habitat

For data simulated from patchy random landscapes, both the non-spatial null model and SECR provided nearly unbiased estimates of realised N with near-nominal confidence interval coverage and similar precision (Table 2). In

923

Table 2. Estimates of expected population size $\bar{\mu}$ and realised population size $\hat{N}$ from spatially explicit capture–recapture compared to three non-spatial estimators of realised population size. Analyses of data simulated under four scenarios for spatial sampling (A–D), and random habitat patches comprising 25% of landscape (Patchy) (see also Table 1 and Fig. 2). Results are summarized as mean relative bias (RB), mean relative standard error (RSE), and coverage of 95% confidence intervals (Coverage). SE in parentheses; 1000 replicates. RB and Coverage are relative to the population size realised in each replicate, except for SECR $\bar{\mu}$, for which RB and Coverage are relative to the expected population size.

Scenario	Estimator	RB	RSE	Coverage
A	M_0 null	−0.068 (0.003)	0.090 (0.001)	0.903
	M_b Zippin	−0.036 (0.009)	0.178 (0.004)	0.906
	M_h jackknife	+0.095 (0.005)	0.112 (0.001)	0.779
	SECR $\hat{N}$	+0.010 (0.003)	0.098 (0.001)	0.940
	SECR $\hat{\mu}$	+0.004 (0.005)	0.152 (0.000)	0.945
B	M_0 null	−0.708 (0.001)	0.096 (0.001)	0.000
	M_b Zippin	−0.700 (0.003)	0.189 (0.005)	0.048
	M_h jackknife	−0.652 (0.002)	0.117 (0.001)	0.000
	SECR $\hat{N}$	+0.025 (0.004)	0.144 (0.000)	0.949
	SECR $\hat{\mu}$	+0.024 (0.005)	0.157 (0.000)	0.957
C	M_0 null	−0.003 (0.002)	0.075 (0.000)	0.949
	M_b Zippin	+0.013 (0.005)	0.133 (0.003)	0.937
	M_h jackknife	+0.145 (0.004)	0.097 (0.001)	0.617
	SECR $\hat{N}$	+0.044 (0.003)	0.082 (0.000)	0.879
	SECR $\hat{\mu}$	+0.046 (0.004)	0.138 (0.000)	0.944
D	M_0 null	−0.505 (0.002)	0.126 (0.001)	0.013
	M_b Zippin	−0.470 (0.007)	0.316 (0.007)	0.303
	M_h jackknife	−0.400 (0.003)	0.112 (0.000)	0.007
	SECR $\hat{N}$	+0.040 (0.007)	0.203 (0.001)	0.933
	SECR $\hat{\mu}$	+0.040 (0.007)	0.212 (0.001)	0.941
Patchy	M_0 null	−0.026 (0.002)	0.059 (0.001)	0.934
	M_b Zippin	−0.019 (0.004)	0.105 (0.003)	0.931
	M_h jackknife	+0.150 (0.003)	0.081 (0.001)	0.467
	SECR $\hat{N}$	−0.004 (0.002)	0.061 (0.001)	0.944
	SECR $\hat{\mu}$	−0.008 (0.014)	0.103 (0.001)	0.311

this respect, the SECR estimates were robust to a strongly non-Poisson distribution of home-range centres. Coverage of the confidence intervals for estimates of expected N was unsatisfactory (31%); as the estimator itself was nearly unbiased the problem lay in underestimation of the sampling variance. This is to be expected from the strongly non-Poisson process model, as we discuss later.

Skink field study

We live-trapped 105 skinks; these were concentrated at the uphill end of the grid (Fig. 3B) where most traps were in the high-cover habitat class (Fig. 3B). Of the three SECR models, the Habitat model was most strongly supported (AICc weight 0.99) and the Null model was greatly inferior (ΔAICc = 102) (Table 3). The inhomogeneous density models Habitat and Qtrend fitted equally well,

Table 3. Comparison of SECR models for variation in the density of skinks across a grid of pitfall traps. np is the number of fitted parameters, including 2 detection parameters; LL is the maximized log likelihood; ΔAICc is the difference in small-sample-adjusted AIC between the current model and the best model. habclass is a 2-level factor; x and y are spatial coordinates.

Model	Formula	np	LL	ΔAICc	AICc weight
Habitat	D~habclass	4	−568.8	0.0	0.99
Qtrend	D~x + y + x² + y² + xy	8	−568.5	8.6	0.01
Null	D~1	3	−620.6	101.5	0.00

but Habitat used fewer parameters. Half-normal detection parameters estimated with the Habitat model were $\bar{g}_0 =$ 0.16 (SE 0.02) and $\hat{\sigma} = 4.4$ m (SE 0.2 m); estimates varied little between models. Despite the differences in AICc, the homogeneous (Null) and inhomogeneous models gave similar estimates of the expected number inside the trapping grid (Fig. 4). Non-spatial estimates of realised N ($\tilde{N} = 119$, 112, 153 for different estimators) were intermediate between estimates from the Habitat model for the trapping grid (95) and for the SECR region of integration (208) (see also Fig. 4).

Simulations showed the homogeneous model to give nearly unbiased estimates of expected N for the region inside the trapping grid when data were generated from the fitted Habitat model (RB −0.03, SE 0.002) or the fitted Qtrend model (RB −0.01, SE 0.003). Extrapolation to the region of integration also gave nearly unbiased estimates in this instance (RB +0.03, SE 0.002 Habitat; −0.04, SE 0.003 Qtrend) and coverage of 95% confidence intervals for realised N was adequate (93.1% Habitat; 90.9% Qtrend).

Discussion

Capture–recapture data from passive detectors such as traps have been used in population studies with little regard to the geographic extent of the target population. Our skink example yielded various conventional estimates of 'population size', but it is meaningless to ask which was
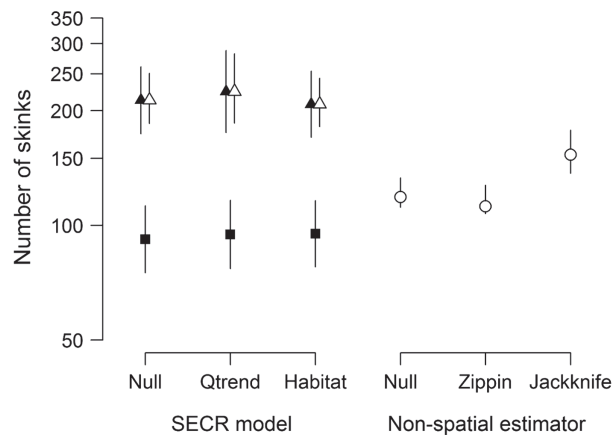
Figure 4. Skink population estimated from SECR models for two hypothetical regions of interest and using conventional non-spatial estimators. SECR estimates relate either to the polygon formed by joining the perimeter traps (squares) or the region within 20 m of at least one trap (triangles) (see also Fig. 3). Region is undefined for non-spatial estimates. Model names follow Table 3. Filled symbols – expected population; open symbols – realised population (not available for smaller region). Bars are 95% confidence limits. Note the log scale.

'correct' because area was not specified. In contrast, spatially explicit methods for population size combine a user-specified geographic region of interest with a fitted model of density. SECR estimates of realised population size were generally less biased than estimates from non-spatial methods and showed adequate precision and confidence interval coverage. Estimates of realised population size were shown to be robust for some severe deviations from the fitted model of home-range centres.

Although SECR modelling is slower than conventional capture–recapture, and demands more from the user, it is the more general method and should be considered whenever a spatially distributed population has been sampled with fixed detectors. The additional complexity is small relative to that faced by existing users of capture–recapture as much of the toolkit for SECR overlaps with that for non-spatial methods and is available in software (temporal, spatial and individual covariates, behavioural response to capture, finite mixture models for unmodelled heterogeneity, AIC-based model selection and model averaging etc.). If both population density and population size are needed they can be estimated from a common SECR model, rather than by fitting separate spatial and non-spatial models to the one data set.

Each simulated spatial scenario represented a situation that might arise in the field. The 'habitat island' scenario (A) would seem to be the one most suited to conventional closed population capture–recapture modelling, as all animals are exposed to detectors. However, central animals are exposed to more detectors than marginal animals, so the probability of detection varies between individuals ($CV(p_i) > 0.2$ in Table 1), and the non-spatial estimates of N are correspondingly biased (Table 2). SECR estimates are free of this particular problem, but heterogeneity from other sources may remain even after spatial effects have been modelled.

Where some individuals in the target population are distant from any detector (scenarios B and D), non-spatial methods fail, but SECR estimators continue to work well. This applies even in the seemingly unlikely case that detectors are scattered in clusters (scenario D), a property that may be used in enhanced sampling designs as discussed later. Under scenarios B and D, the detected individuals were a small fraction of the total in the region of interest ($E(p_i) = 0.22$, 0.30; Table 1), which explains why the estimated variance of realised N was little different from that of expected N.

Scenario C represents a survey covering both occupied and unoccupied areas, between which no distinction can be made in advance (density was zero over 69% of the nominated region). This is a common problem with relict populations of cryptic species, and would be expected to challenge the SECR estimator, which assumed a homogeneous population. The relative lack of bias suggests that SECR estimates of N may be useful even in this situation, as we discuss next.

Inhomogeneous density

Density was strongly inhomogeneous in the skink field example and in our simulations of random landscapes. Skink density could be modelled with the habitat covariate or a quadratic trend surface. It is interesting that the estimate of population size on the trapping grid or in the region of integration from either inhomogeneous model was similar to the corresponding estimate from a homogeneous model. The low bias in simulations from random binary landscapes and from Scenario C suggests this result may apply more widely when sampling spans the region of interest. In general, population size estimates were robust to misspecification of the density model, and a homogeneous model provided reliable estimates.

In simulations of random landscapes the confidence intervals for expected population size showed low coverage, from which we can infer the variance estimates were negatively biased. This is easily explained. The algorithm for generating random landscapes causes the extent of habitat to vary between realisations. This uncertainty is additional to Poisson variation in the number of home-range centres in a given area of habitat. The true variance of N greatly exceeds expectation from a Poisson model – the variance to mean ratio in simulations was about 30 rather than 1.0. Fitting a Poisson process to a particular realisation does not allow inference regarding the variance of the global process. The estimated variance of $\bar{\mu}$ may nevertheless be useful as a biased (probably conservative) estimate of $var(\widehat{N}|N)$ when the latter cannot be calculated directly (e.g. Fig. 4). This situation arises when the region of interest is less than the region of integration and does not include the home-range centres of some detected animals.

Scope of inference and study design

Thus far we have considered an arbitrary region of interest without regard to whether it is one for which inference may reasonably be drawn. Extrapolation beyond the sampled region is risky, especially extrapolation of polynomial or

925

logarithmic trends. Extrapolation of a habitat-based density model beyond the sampled region may be justified in some cases, but extrapolation of polynomial or logarithmic trends is inevitably flawed. When inference is required for a large region it is more appropriate to collect data intensively at a rigorously selected subsample of places.

Conventional capture–recapture for estimating population size is effective only when the entire population is exposed to detectors, as in scenarios A and C. There should not be 'holes' in which animals have little risk of detection (Karanth et al. 2011). This limits the scale at which non-spatial capture–recapture can be used, as comprehensive coverage with a fine grid of traps or other detectors is often prohibitively expensive. Splitting sampling effort among many small grids is not feasible with non-spatial estimators because they are crippled by edge effects. Spatially explicit modelling removes this constraint, as shown by scenario D (see also Efford et al. 2005).

The possibility of dispersed sampling with clusters of detectors raises further design questions, particularly how to achieve spatial representativeness, the optimal size of cluster, and spacing within clusters. Spatially representative designs have been considered extensively in the context of distance sampling (Buckland et al. 2001) and the same principles apply to SECR. Detector clusters may be located at random within the region of interest, but a systematic configuration with a random origin is more spatially representative and avoids potential overlap between clusters. Fewster (2011) describes methods for variance estimation with systematic designs. Unlike distance sampling, SECR uses movements between detectors to estimate the spatial scale of detection. In a clustered design, movements between clusters are infrequent and the method relies on detecting movements within clusters. Spacing of detectors within clusters should be appropriate to the home-range movements of the target species. If a pilot value of the half-normal detection scale σ is available then a spacing of 2σ is suggested. Optimal design of clustered detector layouts is a topic for further research. Appendix 3 outlines options for the analysis of clustered designs.

Extensions

Variants of the SECR methodology for acoustic data (Efford et al. 2009b), and area searches (Royle and Young 2008, Efford 2011) may also be used to estimate population size. Implementation of SECR for open populations has so far been attempted on only a limited scale (Gardner et al. 2010) and further development is needed.

References

Borchers, D. L. and Efford, M. G. 2008. Spatially explicit maximum likelihood methods for capture–recapture studies. – Biometrics 64: 377–385.

Buckland, S. T. et al. 2001. Introduction to distance sampling. – Oxford Univ. Press.

Burnham, K. P. and Overton, W. S. 1978. Estimating the size of a closed population when capture probabilities vary among animals. – Biometrika 65: 625–633.

Burnham, K. P. and Anderson, D. R. 2002. Model selection and multimodel inference: a practical information-theoretic approach, 2nd edn. – Springer.

Chao, A. and Huggins, R. M. 2005a. Classical closed population models. – In: Amstrup, S. C. et al. (eds), Handbook of capture–recapture methods. Princeton Univ. Press, pp. 22–35.

Chao, A. and Huggins, R. M. 2005b. Modern closed population models. – In: Amstrup, S. C. et al. (eds), Handbook of capture–recapture methods. Princeton Univ. Press, pp. 58–87.

Dorazio, R. M. and Royle, J. A. 2003. Mixture models for estimating the size of a closed population when capture rates vary among individuals. – Biometrics 59: 351–364.

Efford, M. G. 2004. Density estimation in live-trapping studies. – Oikos 106: 598–610.

Efford, M. G. 2011. Estimation of population density by spatially explicit capture–recapture analysis of data from area searches. – Ecology 92: 2202–2207.

Efford, M. G. 2012. secr: spatially explicit capture–recapture models. – R package ver. 2.3.2 < http://CRAN.R-project.org/ package = secr >.

Efford, M. G. et al. 2004. Density: software for analysing capture–recapture data from passive detector arrays. – Anim. Biodivers. Conserv. 27: 217–228.

Efford, M. G. et al. 2005. A field test of two methods for density estimation. – Wildlife Soc. Bull. 33: 731–738.

Efford, M. G. et al. 2009a. Density estimation by spatially explicit capture–recapture: likelihood-based methods. – In: Thomson, D. L. et al. (eds), Modeling demographic processes in marked populations. – Springer, pp. 255–269.

Efford, M. G. et al. 2009b. Population density estimated from locations of individuals on a passive detector array. – Ecology 90: 2676–2682.

Fewster, R. M. 2011. Variance estimation for systematic designs in spatial surveys. – Biometrics 67: 1518–1531.

Gardner, B. et al. 2009. Hierarchical models for estimating density from DNA mark–recapture studies. – Ecology 90: 1106–1115.

Gardner, B. et al. 2010. Spatially explicit inference for open populations: estimating demographic parameters from camera-trap studies. – Ecology 91: 3376–3383.

Huggins, R. M. 1989. On the statistical analysis of capture experiments. – Biometrika 76: 133–140.

Johnson, D. S. et al. 2010. A model-based approach for making ecological inference from distance sampling data. – Biometrics 66: 310–318.

Karanth, K. U. et al. 2011. Estimating tiger abundance from camera trap data: field surveys and analytical issues. – In: O'Connell, A. F. et al. (eds), Camera traps in animal ecology. Springer, pp. 97–117.

Otis, D. L. et al. 1978. Statistical inference from capture data on closed animal populations. – Wildlife Monogr. 62: 1–135.

Pledger, S. 2000. Unified maximum likelihood estimates for closed capture–recapture models using mixtures. – Biometrics 56: 434–442.

Pledger, S. 2005. The performance of mixture models in heterogeneous closed population capture–recapture. – Biometrics 61: 868–876.

Rexstad, E. and Burnham, K. P. 1991. User's guide for interactive program CAPTURE. – Colorado Cooperative Fish and Wildlife Research Unit, Fort Collins.

Rivest, L.-P. and Baillargeon, S. 2007. Applications and extensions of Chao's moment estimator for the size of a closed population. – Biometrics 63: 999–1006.

Royle, J. A. and Young, K. V. 2008. A hierarchical model for spatial capture–recapture data. – Ecology 89: 2281–2289.

Royle, J. A. et al. 2009. Bayesian inference in camera trapping studies for a class of spatial capture–recapture models. – Ecology 90: 3233–3244.

Sandland, R. L. and Cormack, R. M. 1984. Statistical inference for Poisson and multinomial models for capture–recapture experiments. – Biometrika 71: 27–33.

Saura, S. and Martínez-Millán, J. 2000. Landscape patterns simulation with a modified random clusters method. – Landscape Ecol. 15: 661–678.

White, G. C. 2005. Correcting wildlife counts using detection probabilities. – Wildlife Res. 32: 211–216.

White, G. C. and Burnham, K. P. 1999. Program MARK: survival estimation from populations of marked animals. – Bird Study 46: S120–S139.

Appendix 1

Bayesian SECR estimation using data augmentation and MCMC

Bayesian implementations of SECR using data augmentation and MCMC are simulation-based (Royle and Young 2008). At each MCMC iteration an integer number of individuals N is proposed to occupy a region of area A; N may vary between the number observed and an arbitrary upper limit set by the analyst (the level of augmentation). This method estimates the posterior distribution of N directly; density is estimated as N/A. It is feasible also to parameterize likelihood-based SECR models in terms of N. However, treating N as a derived parameter of a fitted model for density (the approach in the main paper) is more flexible than including N as a parameter in a likelihood-based model because it allows N to be inferred for regions other than the region of integration.

Bayesian implementations of SECR have not distinguished explicitly between expected N and realised N. In an example considered by Efford (2011) the posterior variance of N from a model with uninformative priors was close to the sampling variance of N from likelihood-based analyses of the same data using a fixed-N (binomial-n) model (i.e. realised N). Further clarification is needed on this point. We note that both the fixed-N and data-augmentation models treat n as a lower bound on N.

Both Bayesian and maximum-likelihood frameworks for SECR include non-spatial models as a special case. In software for likelihood-based estimation (Efford 2012) a non-spatial model is fitted by fixing the spatial scale parameter at a very large value, effectively 'flattening' the detection function. In the Bayesian formulation of Royle et al. (2009) it is simple to omit the term for dependence of detection on distance from the fitted linear model.

Appendix 2

Estimators for the sampling variance of realised N from spatially explicit capture–recapture models

Here we explain in more detail the three variance estimators indicated in the main text and use simulation to assess their performance.

The development of likelihood-based methods for fitting SECR models has emphasized models that implicitly treat N as a Poisson random variable, while admitting the possibility of treating N as fixed (Borchers and Efford 2008) (we focus initially on the number of home-range centres N in the region of integration S). The models differ in the

distribution ascribed to the number of distinct individuals n as shown in the following table, which also defines the parameters p (not to be confused with capture probability) and λ (see main text for other symbols):

Distribution of		
N	n	Parameter
fixed	binomial (N,p)	$p = \int_S D(\mathbf{x}; \phi) p.(\mathbf{x}; \theta) \, d\mathbf{x}/N$
Poisson (μ)	Poisson (λ)	$\lambda = \int_S D(\mathbf{x}; \phi) p.(\mathbf{x}; \theta) \, d\mathbf{x}$

When D is constant, maximizing the likelihood for the fixed-N model yields estimates of D and μ that are the same as those from fitting a Poisson-N model except for possible numerical effects of rounding and spatial discretisation. For fixed-N the maximum-likelihood estimate of D and its asymptotic sampling variance lead directly to estimates of N in a region of integration with area A: $\widehat{N} = A\widehat{D}$, and $\widehat{var}(\widehat{N}|N) = A^2 \widehat{var}(\widehat{D})$. We call this the 'binomial-n' estimate of the sampling variance.

To infer the realised N for a region B other than the region of integration used in the likelihood we start by treating N as a random variable whose expectation follows from the fitted Poisson model i.e. $N \sim \text{Poisson}(\mu)$, where $\mu = \int_B D(\mathbf{x}; \phi) \, d\mathbf{x}$, using notation from the main text. For any realised population we define $\widehat{N} = \bar{\mu}$, and we will use $\bar{m} = \widehat{N} = \bar{\mu}$ to stand for either, where $\bar{m}$ is understood to be simply a function of the data. We wish to estimate $\text{var}(\widehat{N}|N)$.

By the law of total variance

$$\text{var}(\bar{m}) = E_N\{\text{var}(\bar{m}|N)\} + \text{var}_N\{E(\bar{m}|N)\}$$

If $\bar{m}$ is an unbiased estimate of the realised N (i.e. $E(\bar{m}|N) = N$ for particular N) then

$$\text{var}(\bar{m}) = E_N\{\text{var}(\bar{m}|N)\} + \text{var}_N(N)$$

so

$$E_N\{\text{var}(\bar{m}|N)\} = \text{var}(\bar{m}) - \mu,$$

because $N \sim \text{Poisson}(\mu)$. The left hand side is the average of the desired variance over possible values of N. Substituting estimates from a fitted model (main text Eq. 2 and above) for terms on the right hand side, we suggest

$$\widehat{var}(\widehat{N}|N) = \widehat{var}(\bar{\mu}) - \bar{\mu} \tag{A1}$$

as an estimator for the variance of realised N. We call this the 'Poisson' estimate of sampling variance.

For a third estimator of $\text{var}(\widehat{N}|N)$, we note that inference about N is equivalent to predicting a single observation from data (n) and a model (D(.), p.(.)). This suggests a variance estimate based on the mean squared prediction error

(MSPE) (Johnson et al. 2010). Following Eq. 6 of Johnson et al., MSPE is approximately the sum of two terms, one for Poisson variation in the unobserved fraction (given a Poisson distribution of home-range centres), and the other for uncertainty in the model parameters:

$$\text{MSPE}(\widehat{N}) \approx [\widehat{N} - n] + \widehat{\mathbf{H}}^{\mathbf{T}}\widehat{\mathbf{V}}\,\widehat{\mathbf{H}} \qquad (A2)$$

where $\widehat{\mathbf{H}}$ is the estimated gradient of $\widehat{N}$ with respect to β, evaluated at the maximum likelihood estimates.

Simulations

The performance of confidence intervals for N from the fixed-N model has not been assessed previously, and the remaining variance estimators are somewhat ad hoc. We therefore performed simulations to compare the performance of the variance estimators for low- and medium-intensity sampling of small and large populations when the assumptions of the SECR model were satisfied. Computations used the R package secr (Efford 2012) as indicated below.

Home-range centres of 50 and 1000 individuals were simulated uniformly in a square region extending 50 m beyond a square grid of 100 traps at 100-m spacing. Sampling (function 'sim.capthist') was conducted on five notional occasions. Animals could be caught in only one trap per occasion. Probability of capture in a particular trap was a half-normal function of distance from the home-range centre, with spatial scale $\sigma = 50$ m and intercept $g_0 = 0.1$ or 0.2. The resulting sample sizes are shown in Appendix Table 2.1; we note that the first scenario yields very few recaptures and is inherently unlikely to support reliable estimates. The competing-hazard model of Borchers and Efford (2008) was fitted with function 'secr.fit' using a region of integration equal to the known, square region within which the population had been simulated. Both fixed-N and Poisson-N models were fitted. Three variance estimators were applied to each simulated dataset. The binomial variance was the asymptotic variance of expected N from the fixed-N model. Poisson and MSPE variances were computed from the fitted Poisson model using Appendix Eq. A1 and A2 (function 'region.N'). Lognormal 95% confidence limits were calculated as described in the main text. For the Poisson estimator, $\bar{\mu}$ was used as the estimate of N, whereas for MSPE $\widehat{N}$ was computed from Eq. 3 in the main text; there was no evidence that these values differed other than from numerical effects of rounding and discretisation.

The estimated relative bias of $\widehat{N}$ (Appendix Table 2.2) was negligible in all scenarios except the first that combined small population size and low sampling intensity. In that case,

Appendix Table 2.1. Properties of samples from simulated scenarios for population size and detection probability. Mean number of distinct individuals (i.e. first captures) (n), and mean number of recaptures (r). SE in parentheses.

Scenario	n	r
$g_0 = 0.1$, $N = 50$	26.5 (0.1)	8.8 (0.1)
$g_0 = 0.2$, $N = 50$	39.1 (0.1)	27.6 (0.2)
$g_0 = 0.1$, $N = 1000$	529.2 (0.5)	173.8 (0.4)
$g_0 = 0.2$, $N = 1000$	784.4 (0.4)	550.5 (0.8)

Appendix Table 2.2. Estimates of realised population size N from spatially explicit capture–recapture simulated under four scenarios for fixed population size and detection probability. Three variance estimators are compared: (1) Binomial-n, (2) Poisson (Eq. A1), (3) MSPE (Eq. A2). Results are summarized as mean relative bias (RB), mean relative standard error (RSE), and coverage of 95% lognormal confidence intervals (Coverage). SE in parentheses; 1000 replicates; data were inadequate for estimation in 6 replicates of the first scenario. Spatial scale $\sigma = 50$ m throughout.

Scenario	Estimator	RB	RSE	Coverage
$g_0 = 0.1$, $N = 50$	Binomial	0.054 (.010)	0.275 (.003)	0.942
	Poisson	0.093 (.011)	0.281 (.003)	0.950
	MSPE	0.093 (.011)	0.271 (.003)	0.939
$g_0 = 0.2$, $N = 50$	Binomial	0.002 (.004)	0.110 (.001)	0.939
	Poisson	0.022 (.004)	0.107 (.001)	0.925
	MSPE	0.022 (.004)	0.107 (.001)	0.920
$g_0 = 0.1$, $N = 1000$	Binomial	0.004 (.002)	0.057 (.000)	0.954
	Poisson	0.006 (.002)	0.057 (.000)	0.953
	MSPE	0.006 (.002)	0.057 (.000)	0.953
$g_0 = 0.2$, $N = 1000$	Binomial	0.000 (.001)	0.023 (.000)	0.954
	Poisson	0.001 (.001)	0.023 (.000)	0.959
	MSPE	0.001 (.001)	0.023 (.000)	0.959

a few extreme $\widehat{N}$ led to noticeable bias on average, especially for estimates based on the Poisson-n model fit. Despite this problem, confidence interval coverage was near the nominal level throughout. We conclude that all three variance estimators provide acceptable estimates. The Poisson estimator is both simple to compute and flexible, in that the region of interest may differ from region of integration.

Appendix 3

Region of integration and conditional likelihood for clustered designs

There are two options for the region of integration when clusters of detectors are dispersed in a probabilistic design across a large region of interest. Integration may be over the entire region of interest or over a set of disjunct patches, one for each cluster of detectors. In either case, the scope of inference remains the entire region. Fitting a homogeneous Poisson model with a unitary region of integration requires the assumption that spatial variance is Poisson at all scales. This is implausible for large areas, which is a motivation for modelling spatial variation in density with inhomogenous Poisson models. The assumption may also be avoided by combining an empirical estimate of the between-patch variance in n_j (the number of animals detected at cluster j, assuming also that each cluster has the same detector configuration) with a model-based estimate of uncertainty in the detection parameters, assuming homogeneity only within patches. The necessary theory is provided by Buckland et al. (2001). Clusters of detectors are also convenient units for bootstrap variance estimation. The SECR detection model may be fitted separately by maximizing the likelihood conditional on n, and overall density is estimated as $\widehat{D} = n/a(\widehat{\theta})$ where $a = \int_S p.(\mathbf{x}; \theta)\,\mathbf{dx}$ (Huggins 1989, Borchers and Efford 2008). Estimates of population size follow from Eq. 1–4. With sparse designs, n is a small fraction of N so we expect little difference between the computed variances for expected and realized N.